A Hybrid HSVD–CEMD Denoising Framework for Improved Spectral Quality in Proton MRS

Alieh Ahdi (PhD)[1]*, Seyed Kamaledin Setaredan (PhD)[2], Abdol-Hossein Vahabie (PhD)[3]

[1]Department of Biomedical Engineering, University of Eyvanekey, Eyvanekey, Iran
[2]School of Electrical and Computer Engineering, University of Tehran, Tehran, Iran
[3]Cognitive Systems Laboratory, Control and Intelligent Processing Center of Excellence (CIPCE), School of Electrical and Computer Engineering, University of Tehran, Tehran, Iran

ABSTRACT

Background: Magnetic Resonance Spectroscopy (MRS) enables noninvasive assessment of brain metabolites, but is often limited by low Signal to Noise Ratio (SNR) and structured artifacts, such as residual water peaks. Conventional denoising methods, including Hankel Singular Value Decomposition (HSVD) and Empirical Mode Decomposition (EMD), address specific noise types but have complementary limitations.

Objective: This study aimed to develop and evaluate a hybrid HSVD and Complex Empirical Mode Decomposition (CEMD) framework for *in vivo* proton MRS of the Alzheimer's brain.

Material and Methods: This retrospective observational *in vivo* methodological study analyzed single-voxel proton MRS (^{1}H-MRS) data acquired from 20 Alzheimer's patients using a 3T Magnetic Resonance Imaging (MRI) scanner. HSVD was first applied to suppress structured residuals, followed by CEMD to remove stochastic high-frequency noise. Performance was assessed using spectral SNR, residual water amplitude, and metabolite linewidths, and compared with conventional averaging, HSVD-only, and CEMD-only approaches.

Results: The hybrid HSVD+CEMD approach achieved the highest SNR (3.24±1.03), reduced linewidths (18.83±4.11 Hz), and preserved key metabolite peaks, outperforming individual methods.

Conclusion: Combining model-based and data-driven denoising provides robust noise reduction while maintaining spectral fidelity, enhancing reliable metabolite quantification in clinical MRS applications, including Alzheimer's studies.

Keywords

Magnetic Resonance Spectroscopy; Magnetic Resonance Imaging; Brain; Signal Processing, Computer-Assisted; Hankel Singular Value Decomposition (HSVD); Complex Empirical Mode Decomposition (CEMD); Hybrid Denoising; Spectrum Analysis

Introduction

Magnetic Resonance Spectroscopy (MRS) is a powerful noninvasive imaging modality that provides unique biochemical information about living tissues. Unlike conventional Magnetic Resonance Imaging (MRI) methods, which depict structural details, MRS enables the detection and quantification of various metabolites, such as N-Acetylaspartate (NAA), Choline (Cho), Creatine (Cr), and myo-inositol (mI), showing that MRS is particularly valuable in

*Corresponding author: Alieh Ahdi
Department of Biomedical Engineering, University of Eyvanekey, Eyvanekey, Iran
E-mail: a.ahdi@eyc.ac.ir

Received: 30 October 2025
Accepted: 15 June 2026

neuroscience, oncology, and metabolic research, especially for diagnosing and monitoring diseases, such as Alzheimer's, epilepsy, and brain tumors [1-3].

However, the clinical and research potential of MRS is often hindered by the inherently low Signal to Noise Ratio (SNR) of the acquired Free Induction Decay (FID) signals. These FIDs are contaminated by various sources of noise, including thermal noise from the acquisition hardware, physiological noise, such as subject motion and respiration, and structured artifacts, such as residual water peaks or baseline distortions. The presence of noise not only degrades spectral resolution but also impairs the reliability of metabolite quantification, necessitating robust denoising strategies [4-6].

Several denoising approaches have been proposed to improve the quality of MRS signals, such as wavelet-based denoising, Savitzky–Golay filtering, low-rank matrix decomposition, and Empirical Mode Decomposition (EMD)-based techniques. A common baseline denoising strategy is signal averaging [7], in which multiple FID acquisitions are combined to suppress random noise, the scan time lengthens, and subject motion degrades since misalignment introduces artifacts across repetitions rather than their canceling. Beyond averaging, model-based methods, such as Hankel Singular Value Decomposition (HSVD) treat the FID as a superposition of exponentially damped sinusoids. By exploiting the resulting low-rank structure in a Hankel representation, HSVD can separate structured components from the remainder, most notably enabling explicit estimation and removal of residual water and other baseline-related contributions [8]. For these reasons, HSVD is widely used in MRS for water suppression and baseline correction.

Alternatively, adaptive and data-driven methods, such as EMD, have been applied to biomedical signals to separate non-stationary and nonlinear components. EMD decomposes a signal into Intrinsic Mode Functions (IMFs), some of which can be selectively discarded to suppress non-stationary noise. Complex Empirical Mode Decomposition (CEMD) extends the EMD framework to complex-valued signals like MRS FIDs, enabling the preservation of phase and spectral structure during denoising [9, 10].

Other approaches include wavelet-based denoising, which removes noise in the time-frequency domain by thresholding high-frequency wavelet coefficients [11], and Principal Component Analysis (PCA), which extracts dominant patterns across repeated FIDs for subspace-based denoising [12]. More recently, deep learning techniques, such as denoising autoencoders, have been proposed, though they often require large training datasets and are less interpretable [13].

Despite significant advancements in MRS denoising techniques, individual methods often exhibit limitations when applied independently. HSVD has limitations in suppressing high-frequency broadband noise. The HSVD model assumes that the FID can be represented as a small number of exponentially damped sinusoids, which correspond to structured spectral components. However, broadband noise in MRS is typically stochastic and does not follow this low-rank exponential structure [14]. As a result, HSVD is effective for removing structured components, such as residual water and improving the spectral baseline, but random noise components may still remain and degrade the overall signal quality.

Adaptive data-driven methods, such as EMD, have also been explored for MRS denoising. These methods decompose the signal into intrinsic mode functions based on its local oscillatory characteristics. However, EMD can face difficulties when spectral components overlap in frequency, which commonly occurs in MRS, where metabolite peaks are often closely spaced or partially overlapping [15]. In such cases, the decomposition may suffer from mode mixing, where noise and signal components appear within the same intrinsic

mode function. Although CEMD improves certain aspects of the decomposition process, it still inherits limitations when separating strongly overlapping spectral features [16].

These inherent tradeoffs motivate the need for hybrid methods that combine the strengths of model-based approaches like HSVD with adaptive methods like CEMD to achieve comprehensive noise reduction while preserving critical spectral information.

The novelty of our framework lies not merely in combining existing techniques, but in their sequential, purpose-driven deployment. Specifically, HSVD is first applied to explicitly suppress structured artifacts after, which CEMD is used to further attenuate the remaining stochastic noise. This two-stage design is tailored to the complex spectral characteristics of in vivo MRS data. In this work, we propose a novel hybrid denoising framework that combines HSVD and CEMD, aiming to exploit the complementary strengths of both methods. First, HSVD is applied to suppress structured residuals, such as the water peak, by modeling the FID using low-rank exponential bases. Then, CEMD is employed to decompose the residual signal and remove high-frequency, nonstructured noise components. This 2-stage approach improves both spectral fidelity and noise suppression compared to using HSVD or EMD alone. The performance of the proposed method is evaluated on real in vivo brain MRS data acquired from Alzheimer's patients. To evaluate the effectiveness of our proposed hybrid method, we conduct a detailed SNR analysis and compare its performance against each method (HSVD and CEMD), as well as other commonly used denoising techniques such as signal averaging and wavelet thresholding. By quantitatively assessing the SNR improvements and visually inspecting the spectral integrity, we demonstrate that the combined HSVD+CEMD approach yields superior denoising performance while preserving the key metabolic features of the spectrum. The proposed method is thus well-suited for clinical applications, where both accuracy and robustness are essential.

Material and Methods

Data Acquisition

This retrospective observational *in vivo* methodological study analyzed single-voxel 1H-MRS data from 20 clinically diagnosed patients with Alzheimer's disease. Data were acquired at the UBC MRI Research Centre using a 3.0-T Philips Achieva system with an eight-channel head coil [9]. A voxel was placed in the Posterior Cingulate Cortex (PCC) and localized using T1-weighted anatomical imaging. The voxel size was 3.6×2.0×1.5 cm^3 (10.8 cm^3). Spectra were acquired using a Point-RESolved Spectroscopy (PRESS) sequence (Echo Time (TE) / Repetition Time (TR) =31 ms/4000 ms), with water suppression and second-order shimming applied. For each of the twenty patients with Alzheimer's disease, 64 water-suppressed and 16 non-water-suppressed FID signals were acquired.

Conventional Spectral Processing

The conventional approach involved time domain averaging of the 64 water-suppressed FID signals. The averaged FID was subsequently converted to the frequency domain via the Fast Fourier Transform (FFT), resulting in the conventional spectrum. The conventional spectrum served as the baseline for evaluating the performance of the proposed denoising methods. The overall acquisition and spectral processing pipeline are illustrated in Figure 1, including voxel placement, FID acquisition, and the conventional grand spectrum with visible metabolite peaks, such as Total Creatine (tCr), Choline (Cho), and N-AcetylAspartate (NAA).

Proposed Denoising Pipeline: HSVD and CEMD

To enhance spectral quality, we applied a two-stage denoising pipeline to each of the

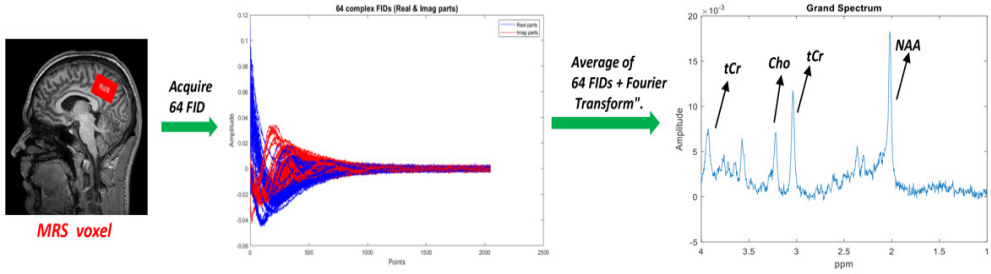

Figure 1: Conventional magnetic resonance spectroscopy (MRS) processing workflow. (Left) Placement of the spectroscopy voxel in the posterior cingulate cortex (PCC). (Middle) Acquisition of 64 complex free induction decay (FID) signals. (Right) Averaging of the 64 FIDs followed by Fourier transformation to generate the conventional grand spectrum, showing metabolite peaks including total creatine (tCr), choline (Cho), and N-acetylaspartate (NAA).

64 individual FID signals before averaging and Fourier transformation. The procedure is summarized below.

1. HSVD

The HSVD is a parametric signal processing method, widely used in MRS to model and remove damped sinusoidal components, such as residual water signals or noise-like artifacts [8, 17].

Let the FID signal be denoted as a complex time-domain sequence: x(n), n = 0, 1,..., N-1.

To apply HSVD, a Hankel matrix $(H)\epsilon C_{L\times M}$ is constructed from x(n), such that each anti-diagonal contains a constant value:

$$H = \begin{bmatrix} x(0)x(1)...x(M-1) \\ x(1)x(2)...x(M) \\ ..... \\ . \\ . \\ x(L-1)x(L)...x(N-1) \end{bmatrix} \quad (1)$$

where $\mathbb{C}$ denotes the set of complex numbers, and L and M represent the number of rows and columns of the Hankel matrix, respectively (such that L+M=N+1).

Singular Value Decomposition (SVD) is then applied:

$$H=U\Sigma V^{H} \quad (2)$$

where Σ denotes a diagonal matrix, whose entries correspond to the singular values. The rank r of the signal subspace is selected based on a singular value threshold or prior knowledge of signal components. The signal is reconstructed using only the r dominant singular values, effectively filtering out the residual water peak and high frequency noise.

From the truncated Hankel matrix, the poles of the signal model are estimated by solving a generalized eigenvalue problem. Each pole corresponds to a damped complex exponential component:

$$x(n) \approx \sum_{k=1}^{r} a_k e^{(-d_k + j\,2\pi f_k)n\Delta t} \quad (3)$$

where a_k, d_k, and f_k are the amplitude, damping factor, and frequency of the k-th component, respectively.

In this study, HSVD was applied to each of the 64 water-suppressed FIDs per subject in a two-stage process. In the first stage, the FID signal was modeled using HSVD with a low rank approximation of r=3 to remove the residual water peak. The fitted signal corresponding to these first three dominant components was subtracted from the original FID to suppress the water signal:

$$FID_{sup}=FID_{orig} - FID_{water\text{-}fit} \quad (4)$$

In the second stage, for noise reduction, HSVD was applied again on the water-suppressed signal using a higher rank model with r=300. The reconstructed signal using the first 300 components was retained, while components corresponding to low-energy noise were discarded. This approach preserves the

metabolite-related signal content while attenuating high-frequency noise:

$$FID_{denoised} = HSVD_r{=}300(FID_{sup}) \quad (5)$$

The choice of HSVD ranks r=5 and r=300 was based on both empirical observations and prior knowledge of the spectral characteristics of MRS signals [18]. In the first step, r=5 was selected to model and remove the dominant water peak, which consistently appeared among the first few singular components across all FIDs. In the second step, r=300 was chosen for noise reduction, as inspection of the singular value spectrum revealed that components beyond this rank contributed negligibly to the total signal energy and were predominantly noise. Retaining the first 300 components preserved the key metabolite information while effectively attenuating high-frequency noise and residual artifacts.

2. CEMD

EMD [19] is an adaptive, data-driven technique for analyzing nonstationary and nonlinear signals. It decomposes a univariate signal s(t) into a finite number of Intrinsic Mode Functions (IMFs) capturing basic oscillatory components inherent to the signal.

A function is considered an IMF if it satisfies two conditions, as follows: 1) the counts of extrema and zero crossings are required to be equal, or their difference must not exceed one, and 2) the mean of the envelopes constructed from the local maxima and minima is required to be zero at all points.

The standard EMD algorithm operates through an iterative sifting procedure. First, all local extrema (both maxima and minima) in the input signal s(t) are identified. Using these extrema, upper and lower envelopes are constructed via cubic spline interpolation. The pointwise mean m(t) of these envelopes is then computed and subtracted from the original signal, yielding d(t) = s(t) − m(t). The resulting component is checked to determine whether it satisfies the Intrinsic Mode Function (IMF) criteria. If the criteria are not met, the sifting steps are repeated on d(t) until convergence. Once an IMF I(t) is finally obtained, it is removed from the signal, and the same sifting procedure is applied to the residual s_residual(t) = s(t) − I(t) to extract subsequent modes.

This iterative process proceeds until the remaining signal becomes monotonic or constant. It should be noted that EMD is inherently formulated for real-valued data. Since FID signals in MRS are complex-valued, standard EMD is not directly applicable. To overcome this limitation, we adopted a CEMD approach [9]. Let s[n] be a complex-valued FID signal. The signal is first transformed into the frequency domain via the Discrete Fourier Transform (DFT), and then separated into its positive and negative frequency components using ideal binary frequency masks:

$$s_+[n] = Real\left(F^{-1}\left\{S\left(\exp(jw)\right).H\left(exp\left(jw\right)\right)\right\}\right) \quad (6)$$

$$s_-[n] = Real\left(F^{-1}\left\{S\left(\exp(jw)\right).H\left(exp\left(-jw\right)\right)\right\}\right) \quad (7)$$

where F^{-1} is the inverse Fourier transform, and the ideal filter is defined as:

$$H\left(exp\left(x\right)\right) = \begin{cases} 1, \omega > 0 \\ 0, \omega < 0 \end{cases} \quad (8)$$

Each of the real-valued components $s_+[n]$ and $s_-[n]$ was then decomposed into a set of IMFs using the EMD algorithm, with the number of IMFs limited to a maximum of 7 to avoid over-decomposition. Importantly, this selection was made based on empirical observation: firstly, three IMFs obtained from EMD on each frequency separated component consistently exhibited prominent peaks in their frequency spectra corresponding to metabolite resonances. These modes were visually identified as containing the desired spectral content while minimizing the contribution of noise and baseline fluctuation. Hence, the final denoised signal was constructed by averaging the first three such modes across FIDs, allowing effective preservation of spectral information.

After selecting the first three IMFs from the components corresponding to positive and negative frequencies, complex-valued IMFs

were reconstructed individually. For each corresponding IMF (i.e., the i-th mode from s_+ and s_-, where i = 1, 2, 3), the analytic representation was formed using the Hilbert transform. Each pair was then combined into a single complex-valued IMF using the following relation:

$$IMFi[n] = (s_+(i)[n] + jH[s_+(i)[n]]) + (s_-(i)[n] + jH[s_-(i)[n]])^* \quad (9)$$

This formulation effectively constructs a complex-valued signal that preserves the spectral symmetry and analytic characteristics of the original FID. The final denoised signal $S_{den}[n]$ was then computed as the sum of these three reconstructed complex IMFs:

$$S_{den}[n] = \sum_{i=1}^{3} IMFi[n] \quad (10)$$

This approach ensures retention of metabolite-related spectral content while effectively reducing residual noise. The overall denoising pipeline, including conventional averaging, HSVD based processing, and CEMD, is summarized in Figure 2, which also illustrates the principle of CEMD decomposition and reconstruction.

Signal Quality Assessment

To quantitatively evaluate the performance of the denoising methods, key metrics, including SNR, residual water peak amplitude, and noise reduction were computed. Spectral SNR was calculated for each method (Conventional, HSVD-only, CEMD-only, and HSVD+CEMD). SNR was defined as the ratio of the height of the NAA peak (approximately 2.0 ppm) to the standard deviation of noise estimated from a noise-only region (e.g., 8.0–9.0 ppm). All SNR values were reported in a linear scale. Detailed results and comparisons based on these parameters are presented in the Results section.

Software and Implementation

All signal processing steps, including HSVD, CEMD, FFT, and SNR calculation,

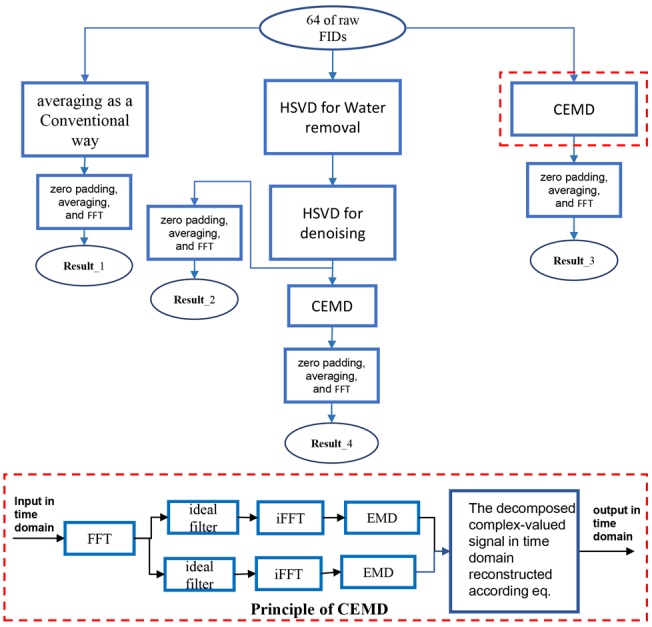

Figure 2: Workflow of the proposed denoising framework. The acquired FID signals are first processed using HSVD for structured artifact suppression, followed by CEMD for stochastic noise reduction. The processed signals are subsequently converted to the frequency domain via the FFT. (FID: Free Induction Decay, HSVD: Hankel Singular Value Decomposition, CEMD: Complex Empirical Mode Decomposition, FFT: Fast Fourier Transform, EMD: Empirical Mode Decomposition)

were implemented in MATLAB R2022a using in-house scripts. The CEMD algorithm was adapted from open-source EMD toolboxes with minor modifications for batch FID processing. All computations were carried out on a conventional desktop system equipped with an Intel Core i7 processor and 32 gigabyte random access memory.

Parameter Validation and Sensitivity Analysis

In our proposed dual-stage HSVD process, two distinct truncation ranks were intentionally employed, each serving a different spectral objective [18]. First HSVD (r=5): a low rank truncation (r=5) was applied to model and remove the dominant structured water resonance. This small rank effectively captures the limited subspace occupied by the strong water peak, ensuring its accurate subtraction without influencing nearby metabolite resonances. Second HSVD (r=300): in a subsequent pass, a higher truncation rank (r=300) was used on the residual signal to attenuate low energy broadband noise components. This rank was empirically determined based on spectral inspection: lower ranks (r<200) led to underfitting and incomplete noise removal, whereas excessively high ranks (r>400) began to overfit and distort narrow metabolite peaks. The chosen r=300 provided an optimal tradeoff between denoising efficacy and spectral fidelity.

This 2 step HSVD configuration allows separation of structured (water) and stochastic (noise) components in a controlled manner, enhancing spectral quality prior to subsequent CEMD refinement.

CEMD IMF Count (K): We evaluated the retention of $K\epsilon\{2,3,4,5\}$ IMFs extracted by CEMD during the stochastic noise filtering stage. Retaining K=2 IMFs resulted in information loss (underfitting), evidenced by the attenuation of key spectral peaks (e.g., in the ppm≈2 region). Conversely, retaining $K\geq4$ IMFs led to the reintroduction of broadband noise artifacts, which negatively impacted the spectral linewidth. By visually inspecting the Fourier spectra of individual IMFs, we confirmed that crucial spectral information was predominantly contained within the first three IMFs. Therefore, the selection of K=3 IMFs was determined as the optimal choice, achieving comprehensive stochastic noise attenuation post water suppression while preserving essential metabolite signals.

Results

Visual Comparison of Spectra

Figure 3 illustrates the preprocessing steps applied to a representative raw FID. In the unprocessed signal and its spectrum (Figure 3a–b), the large water peak dominates the spectral range, obscuring smaller metabolite resonances. Application of HSVD for water suppression (Figure 3c–d) effectively attenuates water-related oscillations. Subsequent noise reduction using HSVD (Figure 3e–f) further improves spectral quality, allowing metabolite peaks to become more clearly visible. All spectra were computed after Fourier transformation of the processed FIDs, with zero-padding to 4096 points to improve spectral resolution.

To better characterize the oscillatory content of the MRS signal, the raw FID was decomposed into IMFs using CEMD. Figure 4 shows the IMFs obtained from a representative raw FID (sample #29). The left panels display the real and imaginary parts in the time domain, while the right panels show their frequency domain spectra (1–5 ppm). Early IMFs capture high-frequency oscillatory components, whereas later IMFs reflect slower baseline fluctuations.

Figure 5 presents the IMFs obtained after HSVD-based water and noise suppression. Compared to the raw FID decomposition, water-related oscillations are largely removed, revealing metabolite-related features more clearly. Inspection of the frequency spectra indicates that the first three IMFs contain

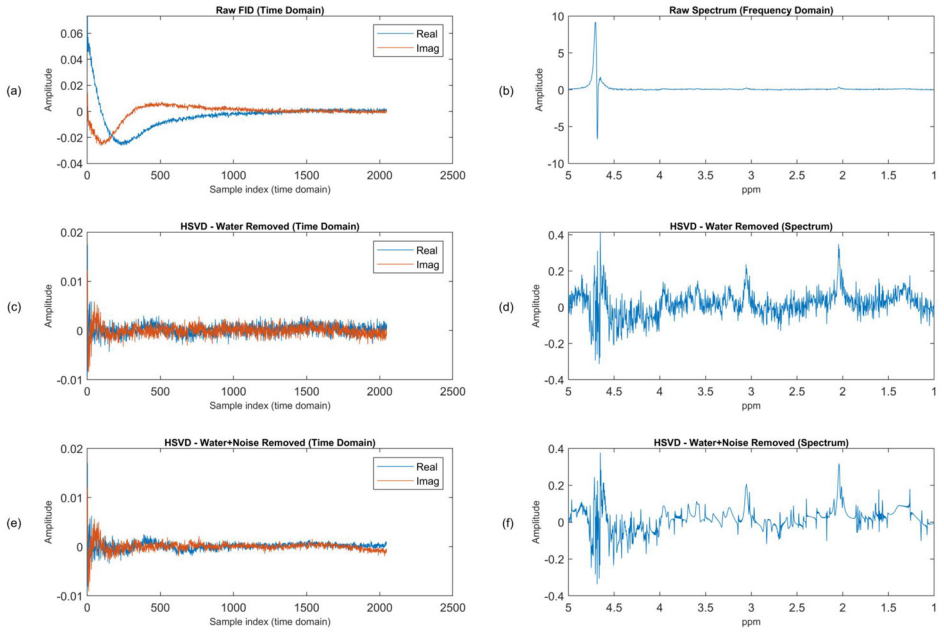

Figure 3: Free Induction Decay (FID) processing at different stages. The left column shows the signals in the time domain (real and imaginary components), while the right column shows the corresponding spectra in the frequency domain (1–5 ppm). (**a**) Raw FID and (**b**) its spectrum. (**c**) FID after water peak removal using Hankel Singular Value Decomposition (HSVD) and (**d**) its spectrum. (**e**) FID after water and noise removal using HSVD and (**f**) its spectrum. Zero padding to 4096 points was applied before the Fourier transformation to improve spectral resolution.

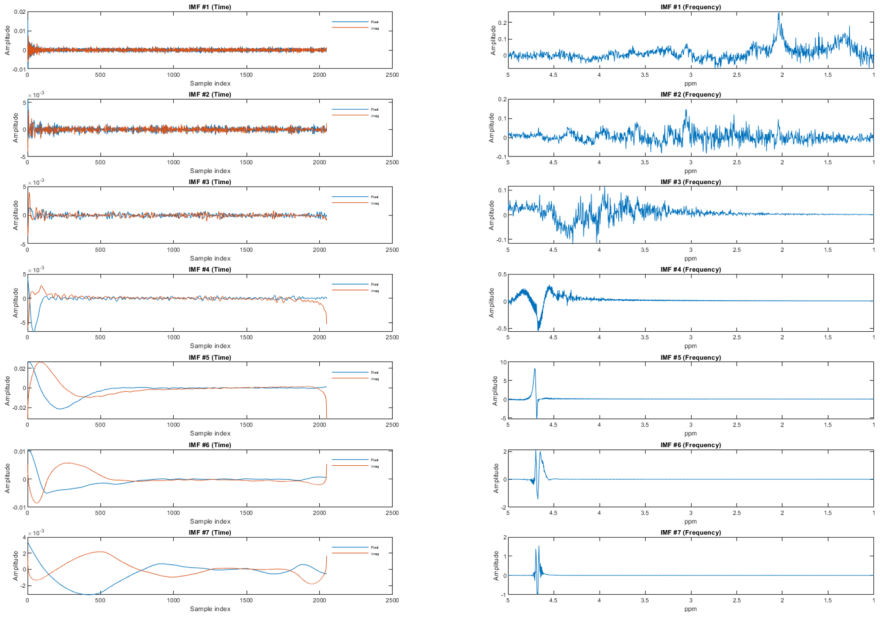

Figure 4: Intrinsic Mode Functions (IMFs) obtained from the raw Free Induction Decay (FID) (sample #29). The left column shows the real and imaginary parts of each IMF in the time domain, while the right column shows their corresponding spectra in the frequency domain (1–5 ppm, after zero padding to 4096 points for improved spectral resolution). This comparison provides the basis for selecting relevant IMFs for subsequent denoising.

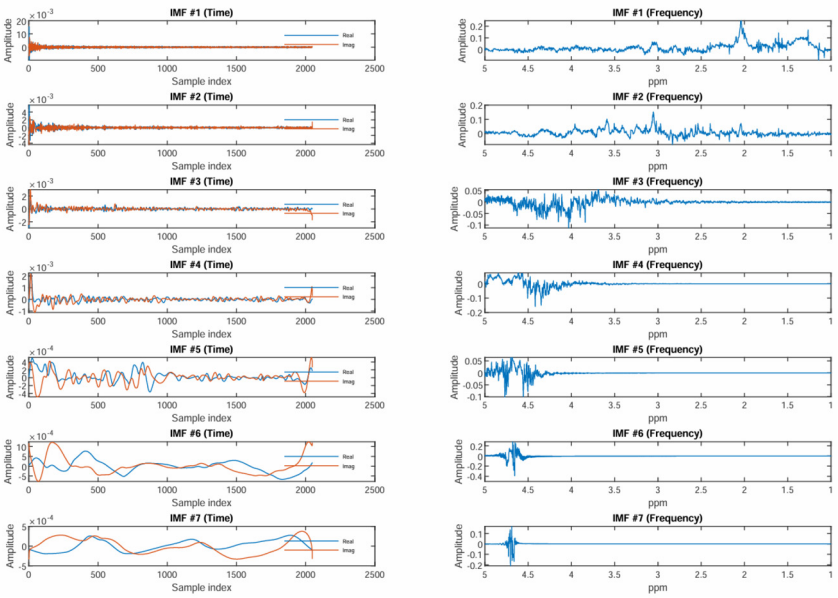

Figure 5: Intrinsic Mode Functions (IMFs) obtained after water suppression and denoising using Hankel Singular Value Decomposition (HSVD) (sample #29). As in Figure 3, the left column shows the time domain components and the right column their spectra. Compared to the raw Free Induction Decay (FID), the dominant water related oscillations are largely removed, revealing metabolite related structures more clearly.

meaningful metabolite peaks (e.g., ~2 ppm for NAA), whereas later IMFs primarily capture residual noise and baseline variations. Accordingly, only the first three IMFs were retained and combined to form the denoised CEMD output.

To qualitatively assess the performance of the different denoising techniques, frequency domain spectra from multiple processing pipelines were compared (Figure 6). Each row corresponds to one denoising approach: (a) HSVD, (b) CEMD, and (c) HSVD+CEMD. In the left panels, the conventional raw spectrum (black) is overlaid with the denoised spectrum (red), illustrating the preservation of metabolite peaks. The right panels display the residual spectrum (blue), computed as the difference between the raw and denoised spectra, highlighting the reduction of residual noise. The spectral window of interest (1–4 ppm) includes major brain metabolites, such as NAA (~2.0 ppm), creatine (~3.0 ppm), choline (~3.2 ppm), and myo-inositol (~3.5 ppm).

In the conventional spectrum, the residual water peak around 4.7 ppm remains prominent, and significant baseline fluctuations and high frequency noise are visible. HSVD-only effectively suppresses the water peak and improves baseline smoothness, although random noise persists, especially between 3–4 ppm. CEMD-only reduces high frequency noise and enhances spectral smoothness, but is less effective against structured artifacts, such as the residual water peak. In some instances, mode mixing slightly distorts metabolite peaks. The hybrid HSVD+CEMD approach combines the strengths of both methods, yielding spectra with minimal water contamination, reduced noise, and preserved metabolite structure. Overall, visual inspection confirms that the two-stage denoising pipeline provides superior spectral clarity compared to individual methods.

These qualitative observations are complemented by quantitative analyses of spectral SNR and residual water peak amplitude, as

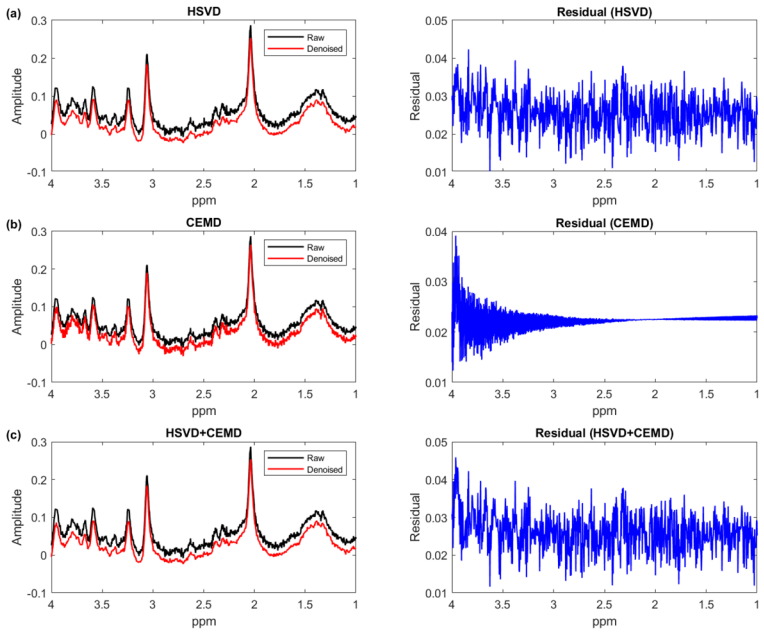

Figure 6: Comparison of raw and denoised spectra using different methods. Each row corresponds to one denoising approach: (**a**) Hankel Singular Value Decomposition (HSVD), (**b**) Complex Empirical Mode Decomposition (CEMD), and (c) HSVD+CEMD. In the left panels, the conventional raw spectrum (black) is overlaid with the denoised spectrum (red). The right panels display the corresponding residual spectrum (blue), computed as the difference between the raw and denoised spectra. The spectral window of interest is shown in the range 1-4 ppm, where major brain metabolites such as N-Acetylaspartate (NAA), creatine (Cr), and choline (Cho) are located. This visualization highlights both the preservation of metabolite signals and the reduction of residual noise after denoising.

detailed in the quantitative SNR evaluation section.

Quantitative SNR Evaluation

1. Quantitative Analysis: Signal to Noise Ratio and Residual Water Suppression

To quantitatively evaluate the performance of the proposed hybrid denoising method, we calculated the SNR for all subjects across the four processing strategies: (1) conventional averaging without denoising, (2) HSVD-only, (3) CEMD-only, and (4) HSVD+CEMD.

Statistical comparisons between methods were performed using two-tailed paired t-tests to assess within-subject differences across denoising strategies, with significance defined as P-value<0.05.

The SNR was computed in the frequency domain for each processed spectrum. Specifically, the SNR was defined as:

$$SNR = \frac{NAA^{A}}{noise^{\sigma}} \qquad (11)$$

where NAA^{A} is the peak amplitude of the NAA resonance at approximately 2.0 ppm, and $noise^{\sigma}$ is the standard deviation of the noise floor measured from a noise-only region (8.0–9.0 ppm) where no metabolite signals are expected.

The quantitative evaluation of spectral quality across different denoising methods is summarized in Table 1. The conventional averaging approach yielded the lowest spectral SNR (2.65±0.71) with incomplete water suppression (100.75±12.26%) and moderate linewidth (22.28±3.57 Hz).

The application of HSVD significantly im-

Table 1: Quantitative metrics for different denoising strategies (mean±SD, N=20)

Method	Spectral-SNR (NAA/σ_noise)	Residual Water (%)	NAA FWHM (Hz)
Conventional	2.65±0.71	100.75±12.26	22.28± 3.57
HSVD-only	3.10±1.28	32.56± 6.73	25.01±2.69
CEMD-only	2.95±1.12	75.45± 30.23	18.41± 4.15
HSVD+CEMD	3.24±1.03	37.45± 86.23	18.83±4.11

SNR: Signal to Noise Ratio, NAA: N Acetylaspartate, σ: noise, Standard Deviation of the baseline noise, FWHM: Full Width at Half Maximum, HSVD: Hankel Singular Value Decomposition, CEMD: Complex Empirical Mode Decomposition

proved SNR (3.10±1.28, *P*-value=0.0133 vs. conventional) and markedly reduced the residual water peak (32.56±6.73%, *P*=0.0035). However, HSVD spectra exhibited broader linewidths compared to the conventional method (25.01±2.69 Hz, *P*-value=0.0009).

CEMD-only denoising achieved a moderate increase in SNR (2.95±1.12) and improved spectral resolution with narrower linewidths (18.41±4.15 Hz, *P*-value<0.001 vs. conventional). Nevertheless, residual water suppression was suboptimal (75.45±30.23%) and significantly worse compared to HSVD (*P*-value=0.0006).

The hybrid HSVD+CEMD method demonstrated the best overall spectral improvement among all tested approaches. It produced the highest SNR (3.24±1.03; *P*-value<0.001 vs. conventional and HSVD) and achieved narrower linewidths (18.83±4.11 Hz; *P*-value<0.001). Although its residual water suppression was moderate (37.45±86.23%), this performance was still significantly better than CEMD alone, which remained lower than HSVD-only (*P*-value<0.001). This pattern reflects the expected trade-off: HSVD excels at removing structured water artifacts, while CEMD is more effective for refining stochastic noise. By combining them sequentially, the hybrid framework maximizes overall spectral clarity even if water suppression is not as strong as HSVD-only.

The HSVD-only method, used as an individual baseline for comparison, demonstrated superior residual water suppression (32.56% vs. 37.45% for HSVD+CEMD, *P*-value<0.001). Conversely, the hybrid method achieved the highest SNR across all comparisons (*P*-value<0.001 versus HSVD-only).

Figure 7 summarizes the distributions of SNR, residual water, and NAA FWHM for all subjects. The hybrid HSVD+CEMD approach shows superior SNR and sharper metabolite peaks while maintaining effective water suppression, illustrating the complementary benefits of combining model-based and data-driven denoising strategies.

These results establish the hybrid HSVD+CEMD pipeline as the most effective denoising strategy overall, motivating further discussion of its implications for clinical MRS.

LCModel-Based Metabolite Quantification Precision

To assess the impact of spectral denoising on metabolite quantification reliability, LCModel analysis was performed on 20 *in vivo* spectra processed using four different pipelines: conventional preprocessing, HSVD-only, CEMD-only, and the proposed HSVD+CEMD framework. Metabolite concentrations and their corresponding Cramér Rao Lower Bounds (CRLBs) were extracted for NAA, Myo-Inositol (mI), and Creatine (Cr). As CRLB reflects the uncertainty associated with metabolite estimation, lower CRLB values indicate higher quantification precision. Table 2 summarizes the mean±standard deviation of CRLB values

across all subjects.

As shown in Table 2, the proposed HSVD+CEMD framework resulted in lower mean CRLB values across all three metabolites compared to the conventional, HSVD-only, and CEMD-only pipelines, indicating improved quantification precision. While HSVD-only and CEMD-only preprocessing led to metabolite-specific reductions in CRLB, their combined application yielded the most stable and consistent metabolite estimates across subjects, as reflected by both reduced mean CRLBs and lower variability.

These results are consistent with the signal to noise ratio and linewidth improvements reported in the quantitative SNR evaluation section, confirming that enhanced spectral quality directly translates into more reliable metabolite quantification.

Discussion

In this study, we evaluated a hybrid denoising approach combining HSVD and CEMD for *in vivo* proton MRS of the Alzheimer's brain. While hybrid denoising strategies utilizing SVD or low rank modeling alongside adaptive techniques like EMD variants have been explored in general signal processing or related NMR fields, our framework introduces a specific, sequential specialization optimized

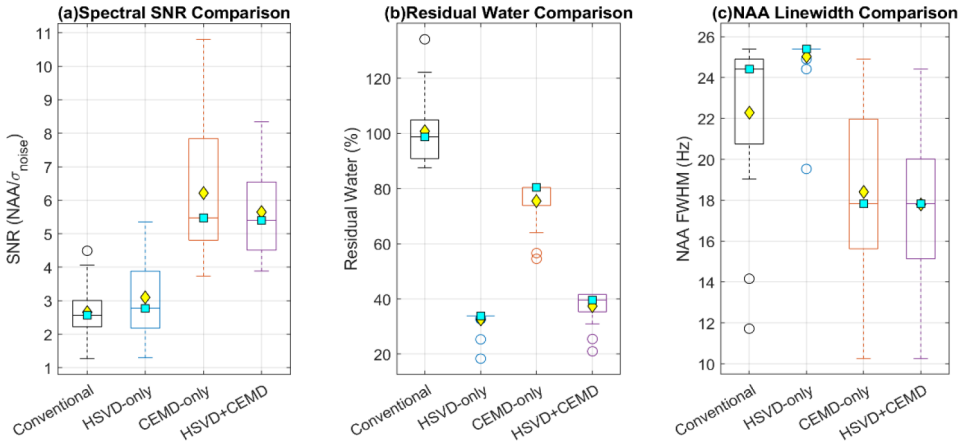

Figure 7: Boxplots show the distribution of (**a**) spectral (Signal-To-Noise Ratio (SNR), N-acetylaspartate (NAA) /σ_noise), (**b**) residual water peak (%), and (**c**) NAA linewidth (Full Width at Half Maximum (FWHM) in Hz) across 20 Alzheimer's patients for four processing strategies: Conventional averaging, Hankel Singular Value Decomposition (HSVD)-only, Complex Empirical Mode Decomposition (CEMD)-only, and HSVD+CEMD

Table 2: LCModel-based metabolite quantification uncertainty expressed as Cramér Rao lower bounds (CRLB, %, mean±SD). (LCModel: Linear Combination of Model spectra)

Method	NAA CRLB (%)	mI CRLB (%)	Cr CRLB (%)
Conventional	1.75±0.68	5.25±2.52	15.4±6.48
HSVD-only	1.75±0.81	10.7±6.81	7.5±9.98
CEMD-only	1.70±0.67	4.75±2.54	13.3±5.24
HSVD+CEMD	1.60±0.94	5.21±2.48	6.5±2.45

NAA: N-acetylaspartate, CRLB: Cramér Rao Lower Bound, mI: myo-inositol, Cr: Creatine, HSVD: Hankel Singular Value Decomposition, CEMD: Complex Empirical Mode Decomposition

for the distinct challenges of *in vivo* MRS. The hybrid methods often focus on simultaneous denoising or employ a less tailored EMD variant. The key novelty is the rigorous two-stage cascade: first, HSVD (r=5) is applied to exploit the low-rank model assumption in order to effectively isolate and suppress the highly dominant, structured residual water peak. This step ensures that the subsequent CEMD stage operates on a baseline that is significantly cleaner than the original signal with structured interference. Second, CEMD is employed on the water-suppressed signal to adaptively decompose and attenuate the remaining stochastic, high-frequency noise, addressing the inherent limitation of HSVD in handling broadband noise. The HSVD→CEMD pipeline differs from parallel approaches and low-rank–diffusion methods [20]. By separating structured (model-based) components from stochastic (data-driven) noise, it achieves better SNR retention and linewidth preservation in our quantitative evaluation on Alzheimer's patient data. The conventional averaging approach reduced random noise through repeated acquisitions but did not address structured artifacts, such as residual water peaks [21]. HSVD primarily targets structured components like the water peak, improving baseline smoothness and partially reducing noise [22]. CEMD, in contrast, achieves an adaptive signal decomposition by extracting intrinsic mode functions, which allows attenuation of high frequency and non-stationary noise components [19, 23].

The hybrid HSVD+CEMD method leverages complementary mechanisms: HSVD removes the dominant structured water component, and CEMD subsequently reduces residual random noise while preserving metabolite peaks. This sequential combination addresses both structured and stochastic noise, providing a robust framework for enhancing MRS data quality. Hybrid denoising approaches have been shown to effectively improve metabolite peak quantification and spectral fidelity in clinical MRS, particularly for metabolites such as NAA. By sequentially targeting structured and stochastic noise components, it enables more reliable quantification of metabolite peaks, which is crucial in studies of Alzheimer's disease and other neurological conditions. For example, Jeon et al. developed a hybrid denoising strategy combining low-rank approximation with a denoising diffusion probabilistic model, significantly improving MRS data quality and reducing scan times [20]. These studies demonstrate the potential of hybrid approaches to enhance MRS data quality, although further validation across diverse datasets and clinical settings is warranted.

While the HSVD+CEMD pipeline delivers the highest overall spectral SNR, Table 1 shows that its residual water suppression performance is quantitatively lower than that of the stand-alone HSVD module (P-value<0.001). Moreover, the standard deviation associated with residual water in the hybrid approach (±86.23%) is substantially larger than for the other configurations. This increased variance suggests that the sequential application is sensitive to minor variations in the initial water component across subjects, such that the secondary CEMD stage may struggle to fully stabilize the remaining artifact. Taken together, these observations indicate that although the hybrid approach successfully optimizes the noise floor (yielding high SNR), the robustness of water removal remains intrinsically linked to the model accuracy of the initial HSVD step. Future refinements should therefore focus on stabilizing the noise suppression stage to ensure more consistent structural artifact removal [5, 17].

Several factors may limit the interpretation and generalizability of the results. The study included 20 Alzheimer's patients, and larger or more heterogeneous cohorts may show different noise characteristics or spectral variability. Data were acquired using single-voxel, water-suppressed ^{1}H MRS at 3T, and variations in voxel size, acquisition parameters (TE/TR, number of averages), or coil configuration

could affect SNR, linewidth, and residual water levels.

Additionally, HSVD ranks and the number of CEMD IMFs were chosen empirically, and may require adjustment for other datasets or protocols. The robustness of the proposed HSVD+CEMD framework is further supported by the sensitivity analysis detailed in the parameter validation and sensitivity analysis section. Our investigation confirms that the selected parameters (r=5, r=300, and K=3) are not arbitrary but represent the precise operational sweet spot balancing artifact removal and spectral fidelity. Specifically, the analysis demonstrated that deviations outside the range (250,350) for r or deviating from K=3 IMFs resulted in a measurable degradation in either SNR or spectral linewidth metrics, providing strong methodological justification for their fixed selection within this 3T MRS protocol.

Residual water suppression also varied across subjects, particularly for CEMD-only and HSVD+CEMD, reflecting motion, hardware, and acquisition differences. Finally, absolute SNR values should be interpreted cautiously, as differences in preprocessing and SNR definitions limit direct comparison across studies.

While the HSVD+CEMD framework demonstrates superior performance over traditional analytical denoising methods (e.g., PCA/SVD) by achieving a better balance between noise suppression and spectral fidelity, we also acknowledge the growing relevance of contemporary state-of-the-art approaches, particularly those based on deep learning or low-rank/diffusion models [13, 24]. The primary objective of this manuscript was to introduce and validate an interpretable, hybrid analytical framework tailored to the inherent spectral structure of low-data MRS. A fair integration and benchmarking of complex, data-intensive DL models would require a dedicated large-scale validation study, typically relying on proprietary training datasets, and is therefore beyond the scope of this initial analytical proof-of-concept. Nevertheless, the framework provides a robust and interpretable baseline that can serve as a reference point for future comparative evaluations against advanced DL-based denoising techniques

While the current study primarily focused on spectral denoising performance and quality improvements, it is important to consider how these enhancements translate into more reliable metabolite quantification. Improvements in spectral SNR and linewidth generally reduce uncertainty in model fitting, which in turn facilitates more stable estimation of metabolites such as NAA, mI, and Cr. This suggests that the HSVD+CEMD framework does not simply clean the spectrum but also strengthens downstream quantification robustness an aspect that is particularly relevant for clinical and research applications where subtle metabolic differences must be detected confidently. The improvement in quantification reliability is critical for clinical MRS studies, as it strengthens confidence in detecting subtle metabolic changes related to neurodegeneration, particularly in the context of Alzheimer's disease.

Although these findings support the utility of the proposed HSVD+CEMD framework, several limitations should be acknowledged explicitly. The study sample consisted of 20 single-site Alzheimer's patients, which may not capture the full variability of noise characteristics across broader or multi-site populations. Acquisition was limited to a single voxel, water suppressed 3T protocol, and the generalizability of the results may vary with different sequences, voxel geometries, or hardware configurations. Additionally, HSVD rank and the number of CEMD IMFs were empirically optimized for this dataset; while sensitivity analysis confirms the stability of these choices within this protocol, they may not represent universally optimal parameters for other scanners or field strengths. Finally, residual water suppression exhibited inter-subject variability, indicating partial dependence on subject-

specific factors, such as motion and hardware stability.

Future work could extend this validation by exploring effects on diagnostic accuracy, assessing robustness across larger multi-site cohorts, and benchmarking against advanced deep learnin- based denoising strategies.

Conclusion

In this study, we introduced a hybrid denoising approach combining HSVD and CEMD for in vivo proton MRS of the Alzheimer's brain. By sequentially targeting structured and stochastic noise components, the method achieved superior spectral quality, evidenced by higher SNR, sharper metabolite peaks, and moderate water suppression compared to conventional averaging, HSVD-only, and CEMD-only approaches. These findings demonstrate that integrating model-based and adaptive data-driven techniques can effectively address complementary noise challenges in MRS, providing a practical framework for clinical applications. Future work will focus on optimizing algorithm parameters, validating the approach in larger and more heterogeneous cohorts, and exploring integration with advanced metabolite quantification and multi-voxel MRS protocols.

Acknowledgment

The authors gratefully acknowledge Dr. Martin McKeown and the staff of the UBC MRI Research Centre for providing access to the MRS data and for their technical assistance.

Authors' Contribution

A. Ahdi conceived and designed the study, implemented the HSVD and CEMD algorithms, conducted signal processing and analysis, and drafted the manuscript. SK. Setaredan supervised the study, provided methodological and technical guidance, and critically reviewed and edited the manuscript. H. Vahhabi contributed to the manuscript review and provided constructive comments to improve the scientific quality. All authors read and approved the final version of the manuscript.

Ethical Approval

This study involving human participants was approved by the University of British Columbia Clinical Research Ethics Board (UBC CREB), Faculty of Medicine (Approval No. H15-02537), and was conducted in accordance with the Declaration of Helsinki.

Informed Consent

The requirement for informed consent was waived by the University of British Columbia Clinical Research Ethics Board (UBC CREB) because the study was retrospective in design and relied on anonymized data.

Funding

This study was conducted without financial support from any public, commercial, or non profit funding agency.

Conflict of Interest

None

References

1. Thomson AR, Hwa H, Pasanta D, Hopwood B, Powell HJ, Lawrence R, et al. The developmental trajectory of 1H-MRS brain metabolites from childhood to adulthood. *Cereb Cortex.* 2024;**34**(3):bhae046. doi: 10.1093/cercor/bhae046. PubMed PMID: 38430105. PubMed PMCID: PMC10908220.
2. Tognarelli JM, Dawood M, Shariff MI, Grover VP, Crossey MM, Cox IJ, et al. Magnetic Resonance Spectroscopy: Principles and Techniques: Lessons for Clinicians. *J Clin Exp Hepatol.* 2015;**5**(4):320-8. doi: 10.1016/j.jceh.2015.10.006. PubMed PMID: 26900274. PubMed PMCID: PMC4723643.
3. Ulmer S, Backens M, Ahlhelm FJ. Basic Principles and Clinical Applications of Magnetic Resonance Spectroscopy in Neuroradiology. *J Comput Assist Tomogr.* 2016;**40**(1):1-13. doi: 10.1097/RCT.0000000000000322. PubMed PMID: 26484954.
4. Kreis R. Issues of spectral quality in clinical 1H-magnetic resonance spectroscopy and a gallery of artifacts. *NMR Biomed.* 2004;**17**(6):361-81. doi:

10.1002/nbm.891. PubMed PMID: 15468083.

5. Near J, Harris AD, Juchem C, Kreis R, Marjańska M, Öz G, et al. Preprocessing, analysis and quantification in single-voxel magnetic resonance spectroscopy: experts' consensus recommendations. *NMR Biomed.* 2021;**34**(5):e4257. doi: 10.1002/nbm.4257. PubMed PMID: 32084297. PubMed PMCID: PMC7442593.
6. Posse S, Otazo R, Dager SR, Alger J. MR spectroscopic imaging: principles and recent advances. *J Magn Reson Imaging.* 2013;**37**(6):1301-25. doi: 10.1002/jmri.23945. PubMed PMID: 23188775. PubMed PMCID: PMC11927461.
7. Provencher SW. Automatic quantitation of localized in vivo 1H spectra with LCModel. *NMR Biomed.* 2001;**14**(4):260-4. doi: 10.1002/nbm.698. PubMed PMID: 11410943.
8. Barkhuijsen H, De Beer R, Van Ormondt D. Improved algorithm for noniterative time-domain model fitting to exponentially damped magnetic resonance signals. *J Magn Reson.* 1987;**73**(3):553-7. doi: 10.1016/0022-2364(87)90023-0.
9. Ahdi A, Ensworth A, Schulz BR, MacMillan E, Mirian MS, Vahabie AH, et al. Assessment of 1H-MRS spectra via multiset canonical correlation analysis and empirical mode decomposition. *Comput Biol Med.* 2025;**187**:109806. doi: 10.1016/j.compbiomed.2025.109806. PubMed PMID: 39923591.
10. Shen G, Zhang L. A complex empirical mode decomposition for multivariant traffic time series. *Electronics.* 2023;**12**(11):2476. doi: 10.3390/electronics12112476.
11. Alexander ME, Baumgartner R, Summers AR, Windischberger C, Klarhoefer M, Moser E, Somorjai RL. A wavelet-based method for improving signal-to-noise ratio and contrast in MR images. *Magn Reson Imaging.* 2000;**18**(2):169-80. doi: 10.1016/s0730-725x(99)00128-9. PubMed PMID: 10722977.
12. Lam F, Liang ZP. A subspace approach to high-resolution spectroscopic imaging. *Magn Reson Med.* 2014;**71**(4):1349-57. doi: 10.1002/mrm.25168. PubMed PMID: 24496655. PubMed PMCID: PMC4051394.
13. Wang J, Ji B, Lei Y, Liu T, Mao H, Yang X. Denoising magnetic resonance spectroscopy (MRS) data using stacked autoencoder for improving signal-to-noise ratio and speed of MRS. *Med Phys.* 2023;**50**(12):7955-66. doi: 10.1002/mp.16831. PubMed PMID: 37947479. PubMed PMCID: PMC10872746.
14. Spear JT, Zu Z, Gore JC. Dispersion of relaxation rates in the rotating frame under the action of spin-locking pulses and diffusion in inhomogeneous magnetic fields. *Magn Reson Med.* 2014;**71**(5):1906-11. doi: 10.1002/mrm.24837. PubMed PMID: 23804212. PubMed PMCID: PMC3919873.
15. Torres ME, Colominas MA, Schlotthauer G, Flandrin P. A complete ensemble empirical mode decomposition with adaptive noise. In IEEE international conference on acoustics, speech and signal processing (ICASSP); Prague, Czech Republic: IEEE; 2011. p. 4144-7.
16. Flandrin P, Rilling G, Goncalves P. Empirical mode decomposition as a filter bank. *IEEE Signal Process Lett.* 2004;**11**(2):112-4. doi: 10.1109/LSP.2003.821662.
17. Pijnappel WW, Van Den Boogaart A, De Beer R, Van Ormondt D. SVD-based quantification of magnetic resonance signals. *J Magn Reson.* 1992;**97**(1):122-34. doi: 10.1016/0022-2364(92)90241-X.
18. Nguyen HM, Peng X, Do MN, Liang ZP. Denoising MR spectroscopic imaging data with low-rank approximations. *IEEE Trans Biomed Eng.* 2013;**60**(1):78-89. doi: 10.1109/TBME.2012.2223466. PubMed PMID: 23070291. PubMed PMCID: PMC3800688.
19. Huang NE, Shen Z, Long SR, Wu MC, Shih HH, Zheng Q, et al. The empirical mode decomposition and the Hilbert spectrum for nonlinear and non-stationary time series analysis. *Proc A.* 1998;**454**(1971):903-95. doi: 10.1098/rspa.1998.0193.
20. Jeon YJ, Nam KM, Park SE, Baek HM. Improving Brain Metabolite Detection with a Combined Low-Rank Approximation and Denoising Diffusion Probabilistic Model Approach. *Bioengineering (Basel).* 2024;**11**(11):1170. doi: 10.3390/bioengineering11111170. PubMed PMID: 39593829. PubMed PMCID: PMC11592133.
21. Govindaraju V, Young K, Maudsley AA. Proton NMR chemical shifts and coupling constants for brain metabolites. *NMR Biomed.* 2000;**13**(3):129-53. doi: 10.1002/1099-1492(200005)13:3<129::aid-nbm619>3.0.co;2-v. PubMed PMID: 10861994.
22. Knight JA, Searles DA, Blaylock RC. The effect of metal chelators on lipid peroxidation in irradiated erythrocytes. *Ann Clin Lab Sci.* 1992;**22**(6):417-22. PubMed PMID: 1456732.
23. Rehman N, Mandic DP. Multivariate empirical mode decomposition. *Proc A.* 2010;**466**(2117):1291-302. doi: 10.1098/rspa.2009.0502.
24. Zhang K, Zuo W, Chen Y, Meng D, Zhang L. Beyond a Gaussian Denoiser: Residual Learning of Deep CNN for Image Denoising. *IEEE Trans Image Process.* 2017;**26**(7):3142-55. doi: 10.1109/TIP.2017.2662206. PubMed PMID: 28166495.